Journal of Quantitative Spectroscopy & Radiative Transfer 205 (2018) 1–6

Contents lists available at ScienceDirect

Journal of Quantitative Spectroscopy & Radiative Transfer

journal homepage: www.elsevier.com/locate/jqsrt

Hyperfine structure of atomic fluorine (F I)

Xiaoxue Huo[a], Lunhua Deng[a,*], L. Windholz[b], Xiuli Mu[a], Hailing Wang[a]

[a] State Key Laboratory of Precision Spectroscopy, East China Normal University, 3663 Zhongshan Road (N.), Shanghai 200062, China
[b] Institute of Experimental Physics, Graz University of Technology, Petersgasse 16, Graz A-8010, Austria

ARTICLE INFO

Article history:
Received 10 July 2017
Revised 21 September 2017
Accepted 21 September 2017
Available online 3 October 2017

Keywords:
Hyperfine structure constants
Atomic fluorine
Atomic spectroscopy

ABSTRACT

A high resolution absorption spectrum of neutral fluorine(F I) was observed around 800 nm using concentration modulation absorption spectroscopy with a tunable Ti : Sapphire laser. The fluorine atoms were produced by discharging the mixed gases of helium and sulfur hexafluoride (SF_6) in a glass tube. Thirty four hyperfine structure (*hfs*) resolved transitions were analyzed to obtain 23 magnetic dipole *hfs* constants *A* for $2p^4(^3P)3s$, $2p^4(^3P)3p$ and $2p^4(^3P)3d$ configurations. The *hfs* constants in $2p^4(^3P)3s$ and $2p^4(^3P)3p$ configurations were compared with those obtained from experiments and calculations. Fifteen constants in $2p^4(^3P)3d$ configuration were reported - to our knowledge - for the first time.

1. Introduction

Atomic fluorine is an important free radical in many chemical processes. Its high resolution structures are helpful to understand the mechanism of fluorine-containing lasers. The experimental *hfs* constants may verify the framework of different theories. This paper studies the high-resolution absorption spectrum of atomic fluorine.

The ground state of fluorine is $1s^22s^22p^5(^2P^o_{3/2})$. The *hfs*-resolved spectra of fluorine were early experimentally studied by Campbell using a Fabry–Perot-interferometer [1]. The $2p^4(^3P)3s$ and $2p^4(^3P)3p$ configurations were studied and their magnetic *hfs* constants *A* were reported. Hocker investigated several transitions in the $2p^4(^3P)3p \rightarrow 2p^4(^3P)3s$ manifold [2]. Measurements were made using a 10.9 m echelle spectrograph providing an overall resolution of about 1:700 000 in the 700 nm wavelength region. They measured hyperfine splittings and broadenings for seven transitions in this region. Three transitions from $2p^4(^3P)3s$ to $2p^4(^3P)3p$ were studied with high-resolution and good frequency accuracy by Tate and Arualiye [3]. They measured the constants *A* using both Doppler-free saturated absorption spectroscopy with an external cavity diode laser and Doppler-limited absorption spectroscopy with a diode laser without external cavity. These authors reported high accurate *hfs* constants for three levels of fluorine. Levy et al. investigated the $2p^4(^3P)3s\,^4P_{5/2} \rightarrow 2p^4(^3P)3p\,^4D_{7/2}$ and $2p^4(^3P)3s\,^4P_{5/2} \rightarrow 2p^4(^3P)3p\,^4D_{5/2}$ transitions of atomic fluorine via laser-induced fluorescence and modulated optical depopulation pumping [4]. The *hfs* constants of the $2p^4(^3P)3s\,^4P_{5/2}$, $2p^4(^3P)3p\,^4D_{5/2}$, and $2p^4(^3P)3p\,^4D_{7/2}$ levels were obtained.

Brown and Bartlett calculated *hfs* separations for the $2p^4(^3P)3s$ and $2p^4(^3P)3p$ configurations [5]. By using the experimental results of Campbell [1], the magnetic moments of the fluorine nucleus were calculated and consistent results were obtained. More recently, Carette et al. calculated the *hfs* constants of fluorine with both no-relativistic and relativistic approach [6]. Using nonrelativistic multiconfiguration Hartree-Fock (MCHF) orbitals, relativity was included in the Breit–Pauli approximation by monoreference (Breit–Pauli, BP) and multireference (MR-BP) approach, or through relativistic configuration interaction calculations using one-electron orbitals built in the Pauli approximation (RCI-P). Fully relativistic multiconfiguration Dirac–Hartree–Fock (MCDHF) and multireference relativistic configuration interaction (MR-RCI) results were also reported. The *hfs* constants for the $2p^4(^3P)3p$ ($^2D^o$, $^4D^o$, $^4P^o$) levels were calculated.

The *hfs* constants of fluorine were mainly reported for levels in $2p^4(^3P)3s$ and $2p^4(^3P)3p$ configurations. There are no *hfs* constants were reported for levels in $2p^4(^3P)3d$ configuration, to the knowledge of the authors. In this work, the levels in $2p^4(^3P)3s$, $2p^4(^3P)3p$ and $2p^4(^3P)3d$ configurations are studied by analyzing the high resolution spectra of fluorine around 800 nm.

2. Experimental setup

The detailed experimental setup was described in previous papers [7,8]. A tunable Ti:sapphire laser (Coherent 899-29) working around 800 nm was used as laser light source. Atomic fluorine was produced by discharging the mixed gases of SF_6 ($\sim$ 8 Pa) and Helium ($\sim$ 200 Pa) in a glass cell. The concentration modula-

* Corresponding author.
E-mail addresses: lhdeng@phy.ecnu.edu.cn, denglunhua@126.com (L. Deng), hlwang@phy.ecnu.edu.cn (H. Wang).

https://doi.org/10.1016/j.jqsrt.2017.09.020
0022-4073/

Table 1
The transitions of F I used to determine the hyperfine structure constants. "No." is our numbering of the investigated transitions. "Obs." (Å) and "Obs." (cm^{-1}) are the c.g. wavelengths (calculated from the wavenumbers) and the observed wavenumbers. "Cal." is the wavenumber calculated from the level's energies cited from the NIST atomic data base [17]. Lines No.24 and 28: see text.

No.	Obs.(Å air)	Obs.(cm^{-1})	Cal.(cm^{-1})	E_L(cm^{-1})	J_L	Term	E_U(cm^{-1})	J_U	Term
1	8844.481	11303.382	11303.36	117308.56	3/2	$^4D^o$	128611.92	3/2	^4F
2	8807.564	11350.759	11350.74	117164.01	5/2	$^4D^o$	128514.75	7/2	^4F
3	8777.723	11389.348	11389.33	117308.56	3/2	$^4D^o$	128697.89	5/2	^2F
4	8737.254	11442.101	11442.08	117164.01	5/2	$^4D^o$	128606.09	5/2	^4P
5	8672.622	11527.372	11527.36	116987.39	7/2	$^4D^o$	128514.75	7/2	^4F
6	8302.388	12041.417	12041.41	116143.58	1/2	$^4P^o$	128184.99	1/2	^4D
7	8298.564	12046.965	12046.95	116040.88	3/2	$^4P^o$	128087.83	5/2	^4D
8	8274.600	12081.854	12081.84	116040.88	3/2	$^4P^o$	128122.72	3/2	^4D
9	8262.455	12099.613	12099.60	116040.88	3/2	$^4P^o$	128140.48	5/2	^2D
10	8232.173	12144.122	12144.11	116040.88	3/2	$^4P^o$	128184.99	1/2	^4D
11	8230.765	12146.199	12146.19	115917.91	5/2	$^4P^o$	128064.10	7/2	^4D
12	8214.713	12169.934	12169.92	115917.91	5/2	$^4P^o$	128087.83	5/2	^4D
13	8208.614	12178.976	12178.95	116040.88	3/2	$^4P^o$	128219.83	3/2	^2D
14	8197.722	12195.157	12195.14	116143.58	1/2	$^4P^o$	128338.72	1/2	^4P
15	8191.234	12204.816	12204.81	115917.91	5/2	$^4P^o$	128122.72	3/2	^4D
16	8179.320	12222.594	12222.57	115917.91	5/2	$^4P^o$	128140.48	5/2	^2D
17	8159.507	12252.273	12252.28	105056.28	1/2	^2P	117308.56	3/2	$^4D^o$
18	8129.287	12297.819	12297.84	116040.88	3/2	$^4P^o$	128338.72	1/2	^4P
19	8126.559	12301.948	12301.92	115917.91	5/2	$^4P^o$	128219.83	3/2	^2D
20	8077.500	12376.664	12376.64	116143.58	1/2	$^4P^o$	128520.22	1/2	^2P
21	8075.505	12379.721	12379.70	116143.58	1/2	$^4P^o$	128523.28	3/2	^4P
22	8040.920	12432.968	12432.96	104731.05	3/2	^2P	117164.01	5/2	$^4D^o$
23	8018.109	12468.339	12468.34	116143.58	1/2	$^4P^o$	128611.92	3/2	^4F
24	8010.494	12480.191	12479.34	116040.88	3/2	$^4P^o$	128520.22	1/2	^2P
25	8007.764	12484.446	12484.47	116040.88	3/2	$^4P^o$	128525.35	5/2	^4F
26	7956.293	12565.210	12565.21	116040.88	3/2	$^4P^o$	128606.09	5/2	^4P
27	7954.056	12568.745	12568.72	116143.58	1/2	$^4P^o$	128712.30	3/2	^2P
28	7952.116	12571.810	12571.04	116040.88	3/2	$^4P^o$	128611.92	3/2	^4F
29	7948.514	12577.508	12577.51	104731.05	3/2	^2P	117308.56	3/2	$^4D^o$
30	7936.315	12596.840	12596.84	115917.91	5/2	$^4P^o$	128514.75	7/2	^4F
31	7930.928	12605.396	12605.37	115917.91	5/2	$^4P^o$	128523.28	3/2	^4P
32	7929.648	12607.432	12607.44	115917.91	5/2	$^4P^o$	128525.35	5/2	^4F
33	7898.586	12657.011	12657.01	116040.88	3/2	$^4P^o$	128697.89	5/2	^2F
34	7879.180	12688.185	12688.18	115917.91	5/2	$^4P^o$	128606.09	5/2	^4P

tion spectroscopy was used to enhance the signal to noise ratio of the absorption spectrum of neutral atomic fluorine. It is an accompanying technique of the velocity modulation spectroscopy [9,10]. The laser frequency was measured by an attached wavemeter and was further calibrated using the absorption spectrum of molecular iodine [11] with a frequency accuracy of 0.007 cm^{-1}.

3. Results and discussion

Atomic fluorine has only one stable isotope, ^{19}F, with a nuclear spin quantum number $I = 1/2$. The coupling with the total angular momentum J of the electron splits the fine structure energy levels into closely spaced doublets with total angular momentum values of $F = J \pm 1/2$. One will obtain three or four hyperfine components for each transition. By fitting the observed *hfs* spectrum, one may obtain the magnetic dipole coupling constant A. Since the nuclear spin quantum number of ^{19}F is $I = 1/2$, the constants B are zero.

A computer program named "Elements" [12,13] was used to estimate the *hfs* constants. The constants A would be carefully optimized till the positions and intensities of the transitions were consistent with the experimental pattern. The rough values of the constants A of the involved levels were determined in this way; the detail procedure can found in Ref. [13].

When the *hfs* constants were roughly determined, a program named "Fitter" [14] was used to get the constants of F I as was done for atomic bromine [8]. The center-of-gravity (c.g.) wavenumbers, the *hfs* constants and the profile were properly determined. One may refer to references [15,16] to get more information concerning "Fitter". The observed transitions were assigned using known levels in the NIST atomic spectra database [17]. The absorption spectra of 34 transitions were assigned as listed in Table 1. Each line is numbered in the table for clarity. The air wavelengths were calculated from the observed wavenumber values using the formula for the refraction index of air given by Peck and Reeder [18]. As can be seen, for line No. 24 the difference between observed and calculated wavenumber is large. The observed structure has three components and looks at the first glance like an hf pattern of F I. But its c.g. wavenumber is 0.85 cm^{-1} higher than the value calculated for this line. Thus we exclude this line from belonging to F I, but we could not identify this transition. A large wavenumber difference is observed also for line No. 28. Observed was most probable an oxygen line with wavenumber 12571.74 cm^{-1} (calculated from the NIST wavelength 7952.16 Å).

As introduced above, the spectra were calibrated using the absorption spectra of molecular iodine with an error of about 0.007 cm^{-1}. The fitted errors of the c.g. wavenumbers are less than 0.001 cm^{-1} and are much smaller than the calibration error. That's to say, the errors of the absolute wavenumbers are mainly coming from the calibration. Thus the fitted c.g. wavenumbers are reported in Table 1 without fitting errors.

Fig. 1 shows the spectrum and fit of transition No. 22 with a calculated c.g. wavenumber of 12,432.96 cm^{-1} (from $2s^2 2p^4(^3P)3s\,^2P_{3/2}$ (104,731.05 cm^{-1}) to $2s^2 2p^4(^3P)3d\,^4D^o{}_{5/2}$ (117,164.01 cm^{-1})). The line shape can be well modeled using the sum of a Gaussian (75%) and a Lorentzian (25%) profile with the same FWMH of about 1350 MHz. The general line width in this study is around 1400 MHz.

Totally, twenty-three levels were studied corresponding to 34 *hfs* - resolved spectra. The graphical level scheme is shown in upper panel of Fig. 2. The transition numbers given in Table 1 are shown in the figure. The transitions No. 24 and No. 28 are labeled

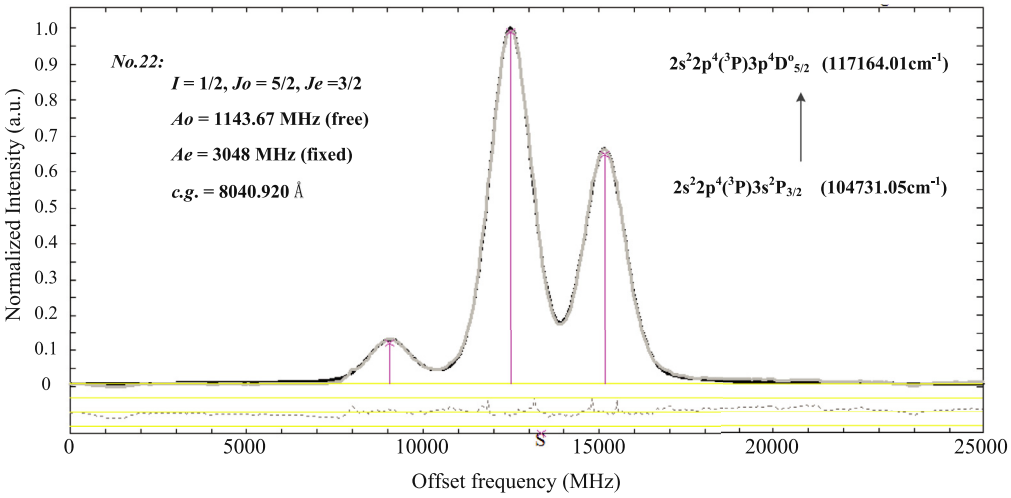

Fig. 1. Hyperfine structure pattern of F I (No. 22 with c.g. wavenumber of 12,432.968 cm $^{-1}$). The components (marked with vertical lines) fitted by the program Fitter are shown. The gray line is the observed absorption spectrum. The black line is the fitted pattern assuming a sum of a Gaussian (75%) and a Lorentzian (25%) profile of the same FWHM (1350 MHz) for each individual component. The lower trace shows the difference between the experimental and the fitted curves. "S" marks the c.g. position.

with dashed lines in Fig. 2. The observed spectra of these two transitions did not fit to the expected pattern and were not used to obtain the *hfs* constants. The line patterns were not fitted independently since they are connected to each other. In general, one known constant should be fixed to fit another unknown constant. The lower panel in Fig. 2 shows the steps to find reliable constants.

Finally, thirty-one transitions labeled with solid lines in Fig. 2 were fitted to obtain the *hfs* constants of the involved levels. In detail, our procedure was introduced as follows:

1. The first step, we fitted the spectra of No. 22 and No. 29 with all constants free. These two fits gave 3054 and 3042 MHz for the constant A of level at 104,731.05 cm^{-1}. The mean value was reported with standard deviation, that is $A_{104,731.05\text{cm}^{-1}}$ = 3048(10) MHz.
2. Then we fitted the spectrum of No. 22 with $A_{104,731.05\text{cm}^{-1}}$ fixed at 3048 MHz. This fit gave $A_{117,164.01\text{cm}^{-1}}$ = 1144(10) MHz for the level at 117,164.01 cm^{-1}. Similarly, No. 29 gave $A_{117,308.56\text{cm}^{-1}}$ = 920(10) MHz. The obtained constants were reported following the uncertainty of the fixed level.
3. When $A_{117,164.01\text{cm}^{-1}}$ = 1144(10) MHz was determined and fixed, the transitions of No. 2 and No. 4 gave $A_{128,514.75\text{cm}^{-1}}$ = 276(10) MHz and $A_{128,606.09\text{cm}^{-1}}$ = −17(10) MHz.
4. Then, the transitions of No. 30 and No. 34 were fitted with their upper levels' constants fixed. These two fits gave an averaged $A_{115,917.91\text{cm}^{-1}}$ = 1054(20) MHz.
5. When the constant of the level 115,917.91 cm^{-1} was determined and fixed, the transitions of No. 11, 12, 15, 16, 19, 31, 32 were fitted to determine constants of their upper levels.
6. The constants of other levels were obtained with the similar procedure, as shown in the lower panel of Fig. 2.

As shown in Fig. 3, transition No. 21 (from 116,143.58 cm^{-1} to 128,523.28 cm^{-1}) was used to confirm the accuracy of the procedure. The constants of its upper (128,523.28 cm^{-1}) and lower (116,14.583 cm^{-1}) levels were determined from different paths using different transitions, as shown in Fig. 2. We simulated the spectrum of No. 21 with fixed constants. In the simulation, the intensity ratio of the less intense components was fixed to 2:1. Good agreement was obtained between simulation and experimental spectrum.

Tables 2 and 3 show the obtained constants of even levels and odd levels, respectively. For a certain level, more than one transition may be observed but not all transitions were used to determine constants, as shown in Fig. 2. For example, nine transitions related to level 115,917.91 cm^{-1} were observed but only two of them (No.30 and No.34) were used to obtain constant of this level dependent on their connection and resolution. Column four lists the numbers of the used transitions.

Table 2 lists the constants of 17 even levels. The *hfs* constants of 15 levels in $2p^4(^3\text{P})3d$ configuration were reported for the first time. The other two levels were studied before and the previously reported constants were cited for comparison. Hocker [2] and Levy [4] gave the hyperfine splitting intervals instead of constants. These splittings were converted into constant A in MHz in the table. For level $3s^2P_{3/2}$, our constant (3048(10) MHz) agrees well with that (3057.9(21) MHz) reported by Tate [3] but disagrees with the other results [1,2,5]. We fitted the spectrum of No. 17 with fixed upper constant and obtained a constant of 1550(200) MHz for level $3s^2P_{1/2}$. Our constant is smaller than 1737.1(40) MHz reported by Tate [3]. The pattern of this line shows a main component and a side component in its low-frequency wing (similar to No. 21, which has a side component in the high frequency wing, cf. Fig. 3). Due to saturation effects, the side component is enhanced in intensity, and the fit result is dependent on the assumed enhancement factor. Thus the A value for the level $2s^22p^4(^3P)3s\ ^2P_{1/2}$ (105,056.28 cm^{-1}) is very hard to determine and can be given only with high uncertainty.

Table 3 lists the constants in $2p^4(^3\text{P})3s$ and $2p^4(^3\text{P})3p$ configurations. Our constants are smaller than those in references [1,5] except $2p^4(^3\text{P})3p\ ^4\text{D}^\text{o}_{3/2}$. Brown et al. [5] calculated the *hfs* constants based on the experimental results of Campbell [1] and no wonder they agree well with each other. Our constants for $2p^4(^3\text{P})3p$ ($^4\text{D}^\text{o}_{7/2}$, $^4\text{D}^\text{o}_{5/2}$) levels are quite close to those reported by Levy [4] obtained from high resolution spectroscopy. Carette et al. [6] reported their relativistic and nonrelativistic calculations. Our constants are close to their calculations using multireference relativistic configuration interaction except level $2p^4(^3\text{P})3p$ ($^4\text{D}^\text{o}_{3/2}$). We found the constant A is 920(10) MHz for level $3p$ ($^4\text{D}^\text{o}_{3/2}$) and our constant is close to their nonrelativistic calculation (930 MHz).

4. Conclusion

The absorption spectra of 34 transitions of neutral fluorine were observed using concentration modulation spectroscopy. The *hfs* constants were obtained for levels in $2p^4(^3\text{P})3s$, $2p^4(^3\text{P})3p$ and $2p^4(^3\text{P})3d$ configurations. The constants of 6 odd levels in

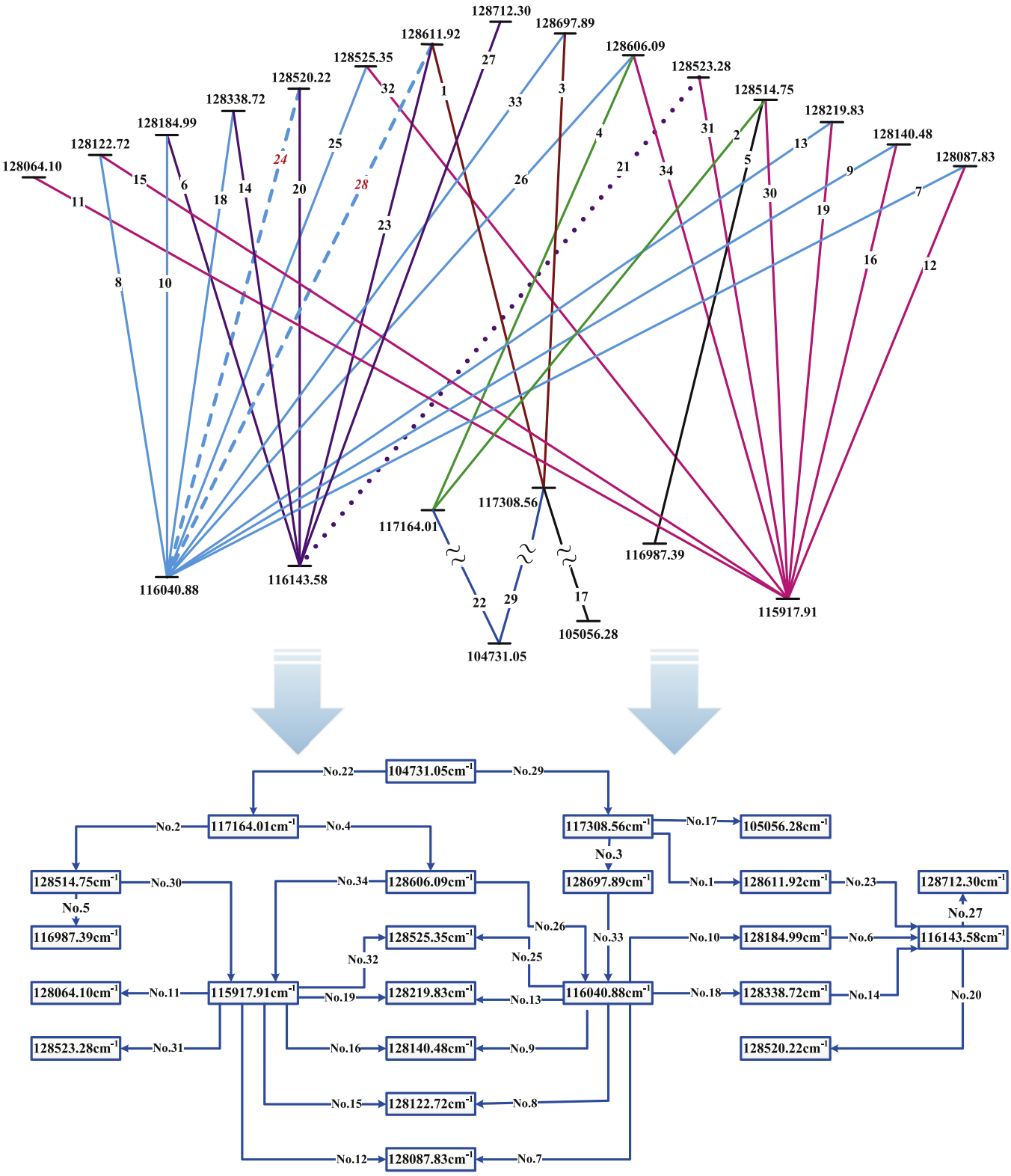

Fig. 2. A level scheme showing the investigated 34 transitions of F I listed in Table 1. Transitions with solid lines were fitted to obtain *hfs* constants. We tried to record transitions No. 24 and No.28 (dashed lines) but observed an un-identified structure and an oxygen-line (see Table 1 and text). Transition No. 21 (dotted line) was used to confirm our results (see Fig. 3). The unit of level energies is cm^{-1}. The lower panel shows the procedure to obtain the *hfs* constants. It begins from the level at 104,731.05 cm^{-1}. The arrows show the successively relationships and are labeled with the transition numbers (see Table 1).

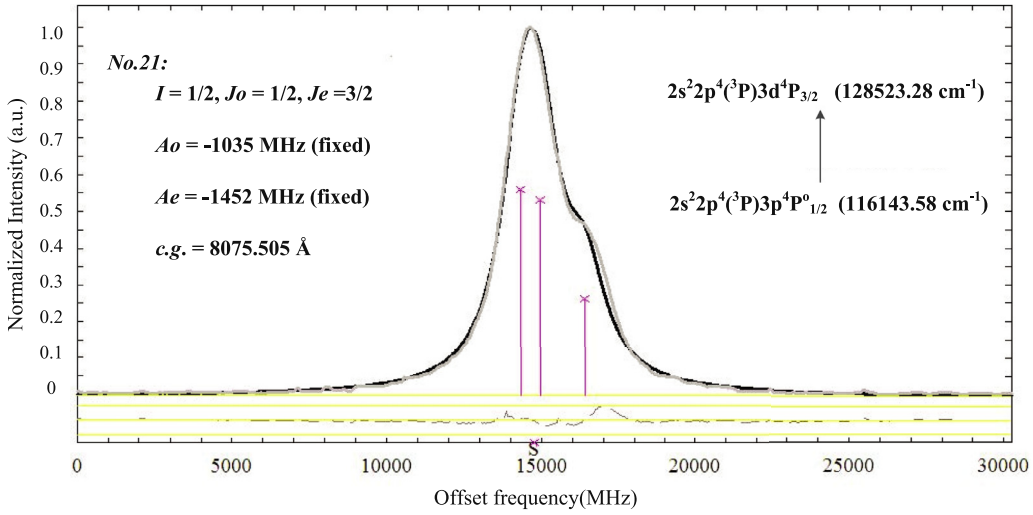

Fig. 3. The upper panel shows the observed spectrum (grey in color) of No. 21 and its simulation curve (black in color) based on the determining constants. In the simulation, the intensity ratio of the less intense components was fixed to 2:1.

Table 2
Hyperfine structure constants A of the even-parity levels of F I. The configuration, level and energy are cited from the NIST atomic spectra database [17]. Column "No." indicates which lines (see No. in Table 1) are used to obtain the given constants.

Configuration	Level	Energy(cm^{-1})	No.	A (MHz)	A (MHz) [1]	A (MHz) [2]	A (MHz) [3]	A (MHz) [5]
$2s^22p^4(^3P)3s$	$^2P_{3/2}$	104731.05	22,29	3048(10)	2100	2700	3057.9(21)	2100
	$^2P_{1/2}$	105056.28	17	1550(200)		2130	1737.1(40)	
$2s^22p^4(^3P)3d$	$^4D_{7/2}$	128064.10	11	793(20)				
	$^4D_{5/2}$	128087.83	7,12	1481(20)				
	$^4D_{3/2}$	128122.72	8,15	2290(50)				
	$^4D_{1/2}$	128184.99	6,10	4541(50)				
$2s^22p^4(^3P)3d$	$^2D_{5/2}$	128140.48	9,16	1046(50)				
	$^2D_{3/2}$	128219.83	13,19	1582(50)				
$2s^22p^4(^3P)3d$	$^4F_{7/2}$	128514.75	2	276(10)				
	$^4F_{5/2}$	128525.35	25,32	304(50)				
	$^4F_{3/2}$	128611.92	1	110(10)				
$2s^22p^4(^3P)3d$	$^2F_{5/2}$	128697.89	3	−190(10)				
$2s^22p^4(^3P)3d$	$^4P_{5/2}$	128606.09	18	−17(10)				
	$^4P_{3/2}$	128523.28	31	−1035(50)				
	$^4P_{1/2}$	128338.72	4	−226(50)				
$2s^22p^4(^3P)3d$	$^2P_{3/2}$	128712.30	27	−498(80)				
	$^2P_{1/2}$	128520.22	20	−2378(80)				

Table 3
Hyperfine structure constants A of the odd-parity levels of F I. The configuration, level and energy are cited from the NIST atomic spectra database [17]. Column "No." indicates which lines (see No. in Table 1) are used to obtain the given constants.

Configuration	Level	Energy (cm^{-1})	No.	A (MHz)	A (MHz) [1]	A(MHz) [4]	A (MHz) [5]	A (MHz) [6]
$2s^22p^4(^3P)3p$	$^4P^o_{5/2}$	115917.91	30,34	1054(20)	1200		1200	1028
	$^4P^o_{3/2}$	116040.88	26,33	1824(20)	2100		2100	1784
	$^4P^o_{1/2}$	116143.58	14,23	−1452(70)				−1555
$2s^22p^4(^3P)3p$	$^4D^o_{7/2}$	116987.39	5	1560(20)	1800	1564(1)	1875	1546
	$^4D^o_{5/2}$	117164.01	22	1144(10)	1290	1148(1)	1300	1127
	$^4D^o_{3/2}$	117308.56	29	920(10)	600		600	850

$2p^4(^3P)3p$ configuration were obtained to verify the previous experimental results and calculations. Seventeen constants were reported for even levels and fifteen of them, belonging to the $2p^4(^3P)3d$ configuration were newly reported.

Acknowledgments

This project was supported by the National Natural Science Foundation of China (Grant No.11674096).

References

[1] Campbell JS. Hyperfeinstruktur im bogenspektrum des fluors. Zeitschr f Physik 1933;84:393. http://10.1007/BF01342219.

[2] Hocker LO. High-resolution study of the helium–fluorine laser. J Opt Soc Am 1978;68:262–5. https://doi.org/10.1364/JOSA.68.000262.

[3] Tate DA, Aturaliye DN. Hyperfine structure intervals and absolute frequency measurement in the $2p^43s^2P_j \longrightarrow 2p^43p^2D_{j'}$ fine-structure multiplet of atomic fluorine by diode laser spectroscopy. Phys Rev A 1997;56:1844. https://doi.org/10.1103/PhysRevA.56.1844.

[4] Levy CDP, Cocolios TE, Behr JA, Jayamanna K, Minamisono K, Pearson MR. Feasibility study of in - beam polarization of fluorine. Nucl Instrum Methods A 2007;580:1571–7. https://doi.org/10.1016/j.nima.2007.07.013.

[5] Brown FW, Bartlett Jr JH. Hyperfine structure of fluorine. Phys Rev 1934;45:527. https://doi.org/10.1103/PhysRev.45.527.

[6] Carette T, Nemouchi M, Li J, Godefroid M. Relativistic effects on the hyperfine structures of $2p^4(^3P)3p\ ^2D^o$, $^4D^o$, and $^4P^o$ in ^{19}F I. Phys Rev A 2013;88:042501. https://doi.org/10.1103/PhysRevA.88.042501.

[7] Wang R, Chen YQ, Cai PP, Lu JJ, Bi ZY, Yang XH, Ma LS. Optical heterodyne velocity modulation spectroscopy enhanced by a magnetic rotation effect. Chem Phys Lett 1999;307(339). https://doi.org/10.1016/S0009-2614(99)00562-X.
[8] Ni X, Deng LH, Wang HL. Hyperfine structure constants of atomic bromine (br i). J Quant Spectrosc Radiat Transf 2017;196:165–8. https://doi.org/10.1016/j.jqsrt.2017.04.013.
[9] Gudeman CS, Megemann MH, Pfaff J, Saykally RJ. Velocity-modulated infrared laser spectroscopy of molecular ions: the ν_1 band of HCO^+. Phys Rev Lett 1983;50:727–31. https://doi.org/10.1103/PhysRevLett.50.727.
[10] Stephenson SK, Saykally RJ. Velocity modulation spectroscopy of ions. Chem Rev 2005;105:3220–34. https://doi.org/10.1021/cr040100d.
[11] Gerstenkorn S., Vergés J., Chevilard J.. Atlas du spectre d'absorption de la molècule d'iode (11000 - 14000 cm^{-1}) (orsay: CNRS II). 1982.
[12] Windholz L, Guthöhrlein GH. Classification of spectral lines by means of their hyperfine structure. Application to Ta I and Ta II levels. Phys Scr 2003:T105:55C60. http://iopscience.iop.org/1402-4896/2003/T105/008.
[13] Windholz L. Finding of previously unknown energy levels using fourier - transform and laser spectroscopy. Phys Scr 2016;91(114003). https://doi.org/10.1088/0031-8949/91/11/114003.
[14] Guthöhrlein G.H.. Program package "Fitter", 1998, (unpublished), Helmut-Schmidt-Universität, Universität der Bundeswehr Hamburg, Holstenhofweg 85, d-22043 Hamburg, Germany. The program code can be obtained from G.H. Guthöhrlein (g.h.g@hsu-hh.de) or L.Windholz (windholz@tugraz.at).
[15] Sobolewski LM, Binder T, Güney C, Gamper B, Kwela J, Windholz L. Laser induced fluorescence and optogalvanic spectroscopy applied to find previously unknown energy levels of La I and studies of their Zeeman structure. J Quant Spectrosc Radiat Transf 2017;200:108–12. https://doi.org/10.1016/j.jqsrt.2017.06.006.
[16] Stefanska D, Furmann B. Hyperfine structure of the odd-parity configuration $4f^9 5d$ in singly ionized terbium. J Quant Spectrosc Radiat Transf 2017;200:113–24. https://doi.org/10.1016/j.jqsrt.2017.06.011.
[17] Kramida A., Ralchenko Y., Reader J. NIST ASD Team 2015. NIST atomic spectra database (ver.5.3),[online]. available:[2016,november 21]. national institute of standards and technology, gaithersburg, MD.
[18] Peck ER, Reeder K. Dispersion of air. J Opt Soc Am 1972;62:958–62. https://doi.org/10.1364/JOSA.62.000958.